Nanoscale

Accepted Manuscript

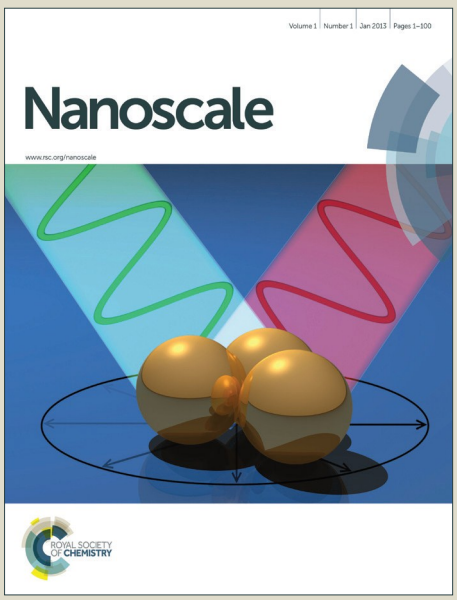

ROYAL SOCIETY OF CHEMISTRY

www.rsc.org/nanoscale

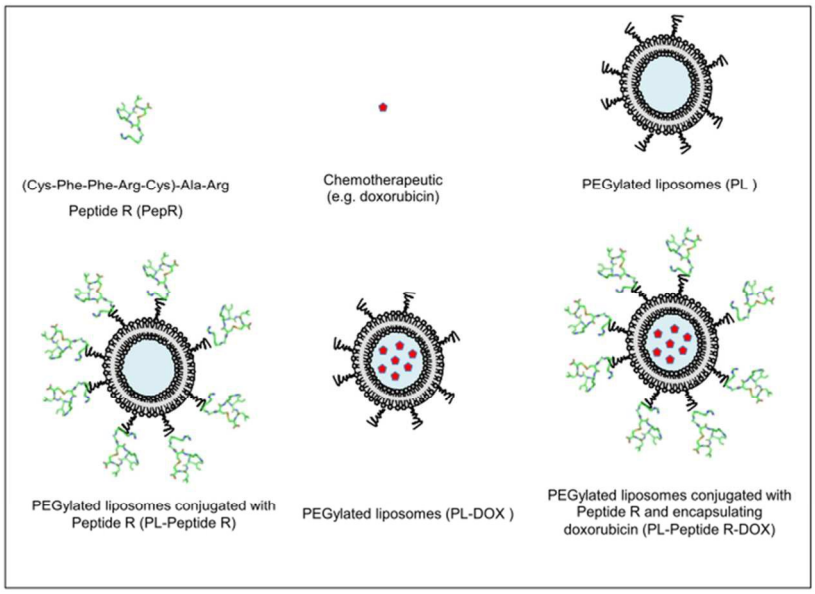

Figure 1

46x34mm (600 x 600 DPI)

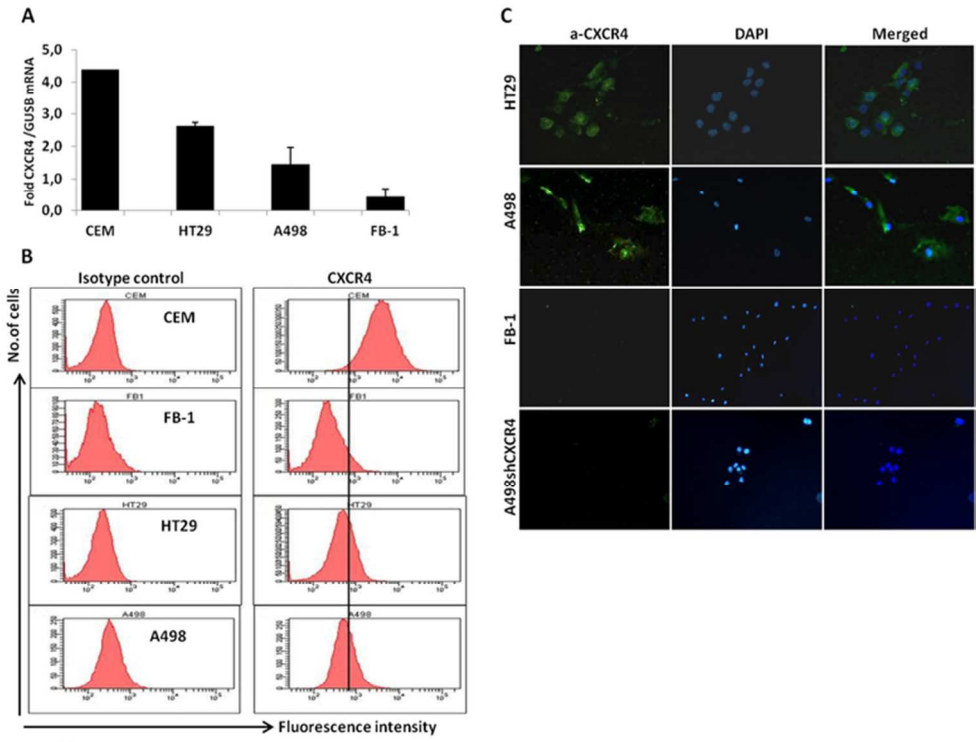

Figure 2

67x52mm (300 x 300 DPI)

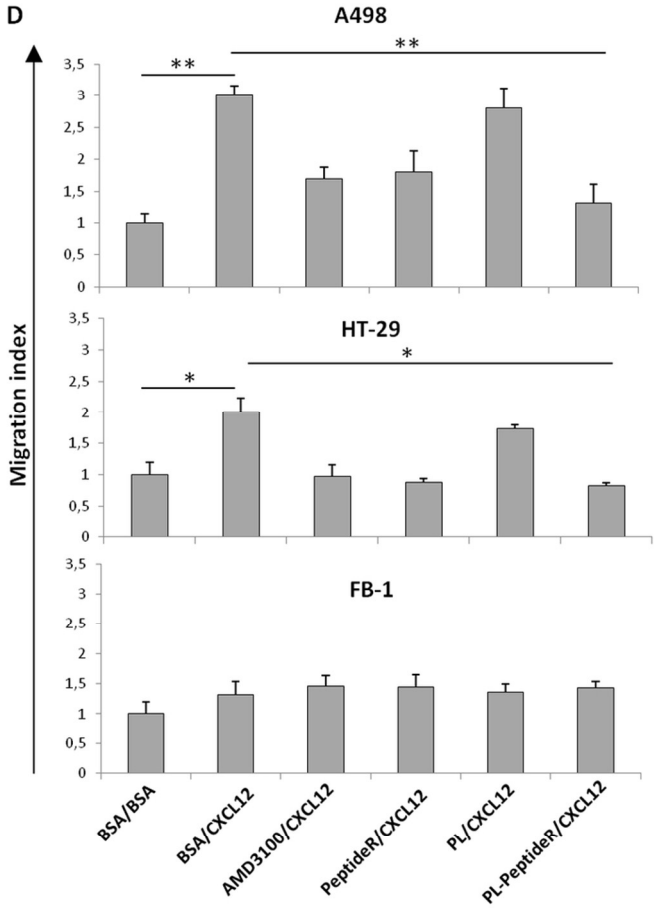

Figure 2

47x45mm (600 x 600 DPI)

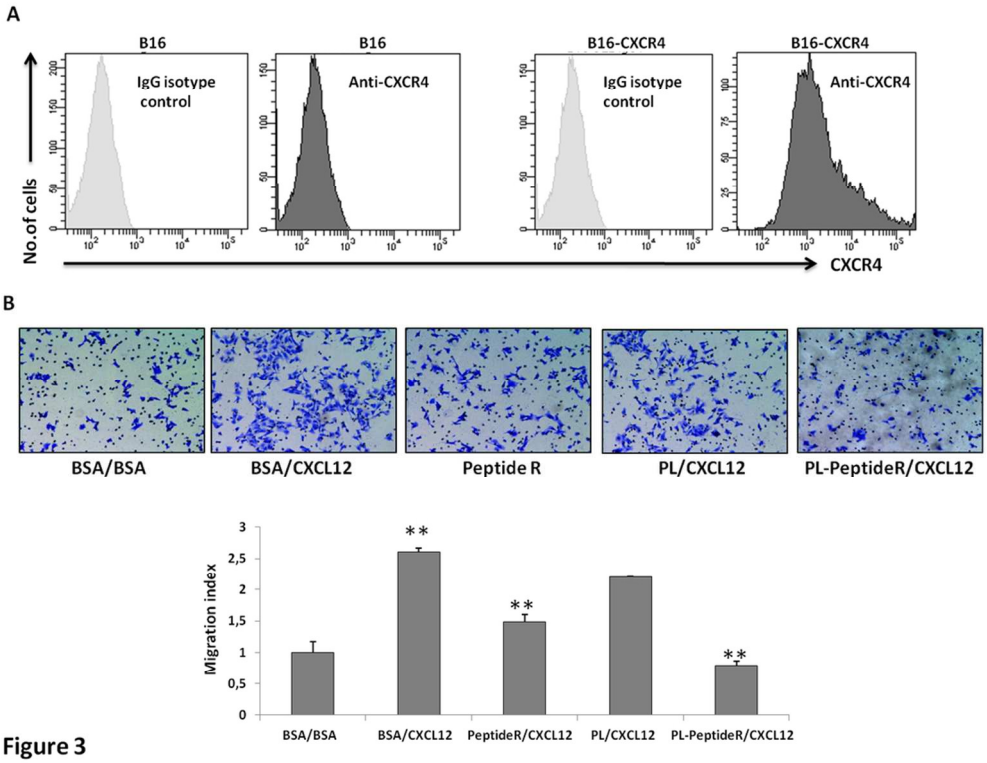

Figure 3

47x36mm (600 x 600 DPI)

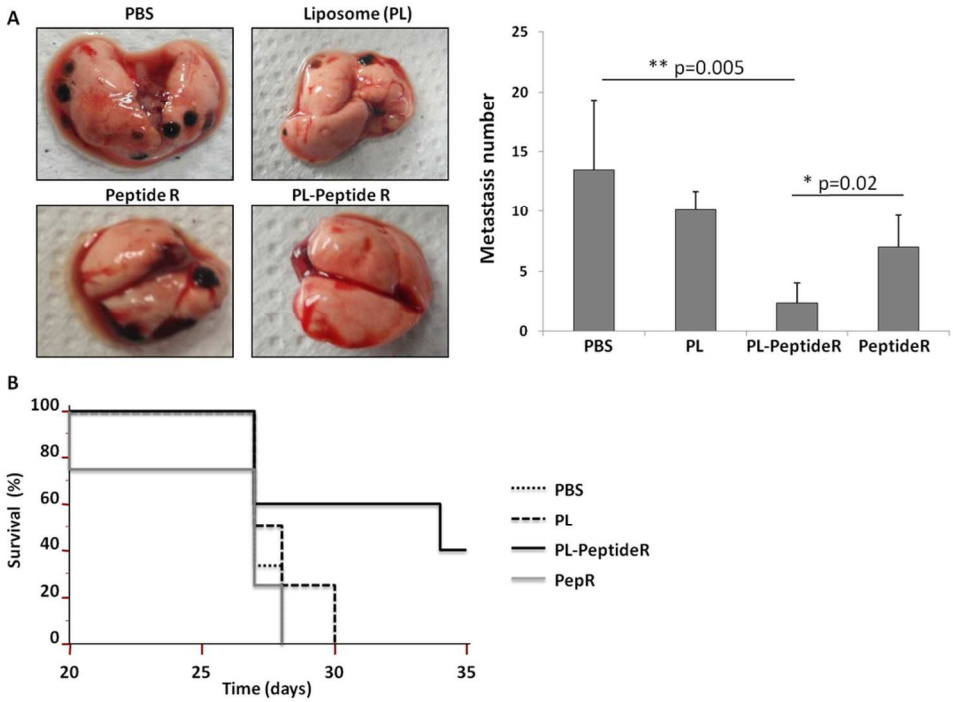

Figure 4

47x35mm (600 x 600 DPI)

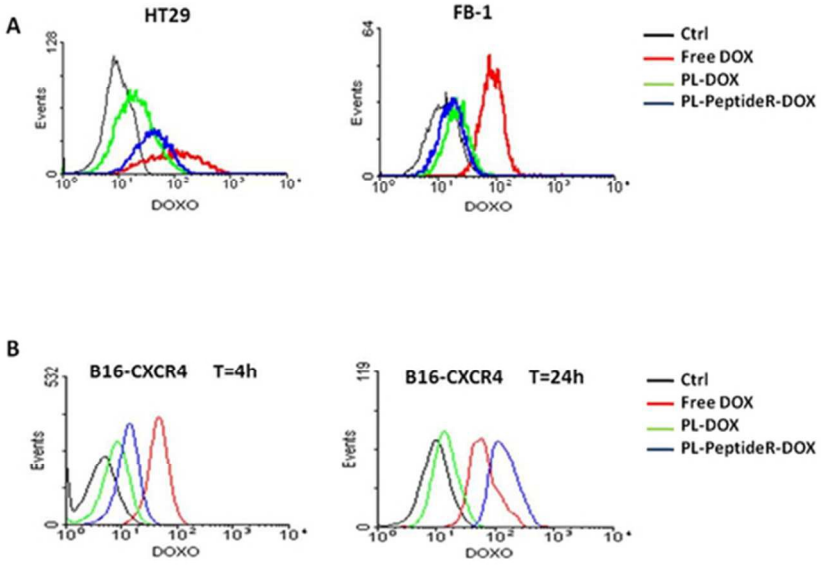

Figure 5

53x40mm (300 x 300 DPI)

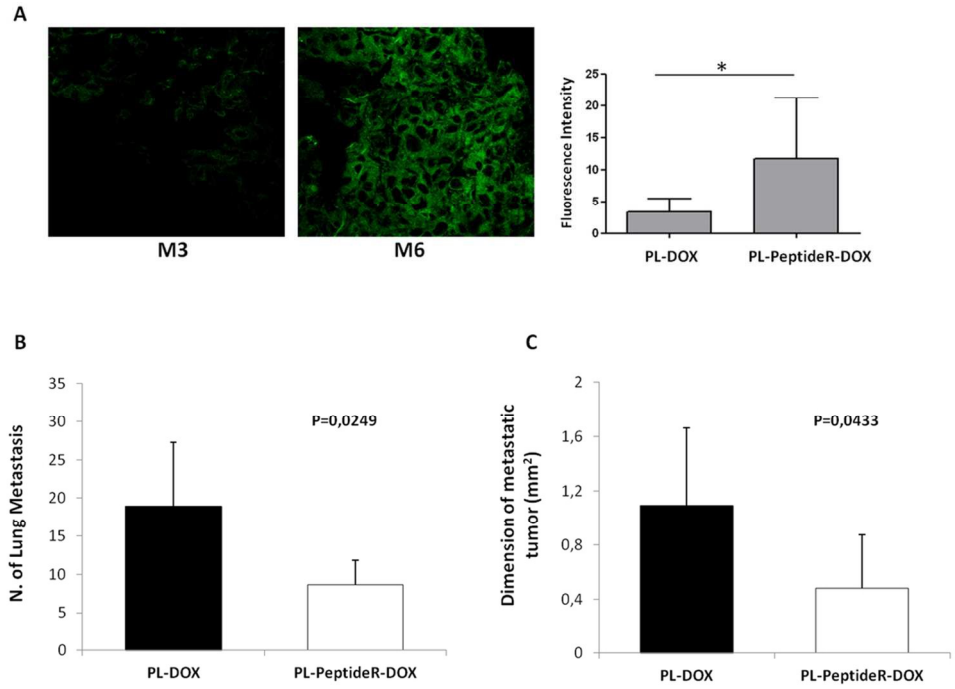

Figure 6

51x38mm (600 x 600 DPI)

CXCR4-antagonist Peptide R- liposomes for combined therapy against lung metastasis

Caterina Ieranò[1], Luigi Portella[1], Sara Lusa[2], Giuseppina Salzano[2,6], Crescenzo D'Alterio[1], Maria Napolitano[1], Maria Buoncervello[4], Daniele Macchia [4], Massimo Spada [4], Antonio Barbieri[3], Antonio Luciano[3], Maria Vittoria Barone[7], Lucia Gabriele[4], Michele Caraglia[5], Claudio Arra[3], [#] Giuseppe De Rosa[2],[#]Stefania Scala[1]

[1]Molecular Immunology and Immuneregulation, [3]Animal Facility,

Istituto Nazionale per lo Studio e la Cura dei Tumori, Fondazione "G. Pascale"-IRCCS-Italy.

[2]Department of Pharmacy, University of Naples Federico II, Via D. Montesano 49, 80131, Naples, Italy.

[4]Department of Hematology, Oncology and Molecular Medicine, Istituto Superiore di Sanità, Viale Regina Elena 299, 00161,Rome, Italy.

[5]Department of Biochemistry, Biophysics and General Pathology, Second University of Naples, Via L. De Crecchio 7, 80138, Naples, Italy.

[6]Center for Pharmaceutical Biotechnology and Nanomedicine, Northeastern University, 360 Huntington Ave, Boston, MA, USA.

[7]Department of Translational Medical Science and European Laboratory for the Investigation of Food Induced Disease (ELFID), University of Naples, Federico II, Via S. Pansini 5, 80131, Naples, Italy.

 # The two authors equally contributed

Keywords: CXCR4, Liposomes, Drug delivery, Cancer

Correspondence: Stefania Scala, M.D., Ph.D

Head Molecular Immunology and Immuneregulation, Functional Genomics

Istituto Nazionale per lo Studio e la Cura dei Tumori, Fondazione “G. Pascale”-IRCCS-Italy.

Via Semmola, Naples

80131. ITALY

Tel +39-081-5903678; fax +39-081-5903820

Mobile +39-3803140318

s.scala@istitutotumori.na.it ; s.scala@gmail.com

Correspondence: Giuseppe De Rosa, Ph.D.

Department of Pharmacy,

University of Naples, Federico II,

Via D. Montesano 49, 80131, Naples, Italy.

Tel +39 0 81678666

gderosa@unina.it

Abstract

The chemokine CXCL12 activates CXCR4, initiating multiple pathways that controls immune cell trafficking, angiogenesis and embryogenesis; CXCR4 is also overexpressed in multiple tumors affecting metastatic dissemination. While there has been great enthusiasm for exploiting the CXCR4-CXCL12 axis as a target in cancer therapy, to date the promise has yet to be fulfilled. A new class of CXCR4-antagonist cyclic peptides was recently developed and the compound named Peptide R was identified as the most active. With the intent to improve efficacy and biodistribution of Peptide R, stealth liposomes decorated with Peptide R were developed (PL-Peptide R). *In vitro* PL-Peptide R efficiently inhibited CXCR4-dependent migration and *in vivo* significantly reduced lung metastases and increased overall survival in B16-CXCR4 injected C57BL/6 mice. To evaluate if PL-Peptide R could also be a drug delivery system for CXCR4 expressing tumors, the PL-Peptide R was loaded with doxorubicin (DOX) (PL-Peptide R-DOX). PL-Peptide R-DOX efficiently delivered DOX to CXCR4 expressing cell lines with a consequent decrease in the DOX IC_{50} efficient dose. In vivo, B16-CXCR4 injected C57BL/6 mice treated with PL-Peptide R-DOX developed fewer lung metastases compared to PL-DOX treated mice. This work provides the proof-of-concept to prevent metastasis by using combined nanomedicine.

Introduction

The chemokine receptor CXCR4 is a seven transmembrane G protein coupled receptor (GPCR) expressed on immune cells including monocytes, B cells and naive T cells in peripheral blood. Its ligand, CXCL12, is a pleiotropic chemokine widely expressed in multiple organs such as brain, lung, colon, heart, kidney, liver and bone marrow, where it acts as a chemoattractant for immature and mature hematopoietic cells. CXCR4 is also overexpressed on tumor cells, where, upon binding to its ligand CXCL12, plays a critical role in the invasion and metastasis in solid and hematological cancers [1-8]. CXCL12 promotes migration of CXCR4 overexpressing tumor cells and increases metastasis rate[9]. Although CXCR4 is an amenable therapeutic target [10, 11] it is actively addressed only in hematopoietic stem cells (HSC) where the Food and Drug Administration (FDA) approved the CXCR4 antagonist Plerixafor (AMD3100) as mobilizing agent in Myeloma and Non-Hodgkin Lymphoma (NHL) patients undergoing to autologous bone marrow transplantation [12, 13]. Although Plerixafor shows anti-metastatic potential in preclinical studies, its toxicity profile limits a long-term administration as required for cancer therapy [14]. Several CXCR4 antagonists are in development [15-17] but only a few are targeting solid tumors [18]. A new family of CXCR4 antagonists was developed. Based on a rational design, a three-aminoacids motif was identified in the CXCL12 ligand receptor-binding region (RFF) and, in the reverse orientation, a structural overlapping motif (WHR) occurred in vMIP-II, an inhibitory chemokine herpes virus 8 (HHV8) secreted. The two regions, in one orientation in activating CXCL12 and in the opposite orientation in the inhibitory chemokine vMIPII inspired a small peptidic library focused on these two sequences[19-20]. The CXCL12-mimetic Peptide R (Arg-Ala-[Cys-Arg-Phe-Phe-Cys]), was the most effective CXCR4 antagonist in *in vivo* models and thus further developed [20]. Despite Peptide R treatment efficiently reduced lung metastasis, peptides are generally rapidly degraded in biological fluids and display a nonspecific distribution into the body that may cause long-term immune system side effects [21, 22].

To increase the peptides bioavailability, conjugation with polymer or encapsulation in nanocarrier have been pursued [23-26].

In this study, stealth liposomes decorated with Peptide R with a combined function were developed: to increase specific anti-metastatic efficacy of Peptide R by tumor targeting [27, 28] and to achieve a new drug delivery system targeted against CXCR4-overexpressing tumor cells.

Material and methods

Materials

1,2-dipalmitoyl-sn-glycero-3-phosphocholine (DPPC) and [N-(Carbonyl-methoxypolyethylenglycol-2000)-1,2-distearoyl-sn-glycero-3-phosphoethanolamine, sodium salt] (DSPE-PEG2000) were purchased from Lipoid GmbH (Cam, Switzerland). 1,2-distearoyl-sn-glycero-3-phosphoethanolamine-N-[maleimide(polyethylene glycol)-2000] (ammonium salt) (DSPE-PEG2000-Mal) was obtained from Avanti Polar Lipids (Alabaster, Alabama, USA).

Doxorubicin hydrochloride (DOX), cholesterol (Chol), sodium chloride, [4-(2-Hydroxyethyl) piperazine-1-ethanesulfonic acid, N-(2-Hydroxyethyl) piperazine-N'-(2-ethanesulfonic acid)] Hepes, ethylenediaminetetraacetic acid (EDTA), sodium citrate, potassium chloride, 2-iminothiolane hydrochloride (Traut's), citric acid, Sepharose CL4B and Sephadex G-25 were purchased from Sigma Chemical Co. (St. Louis, Mo, USA). Acetonitrile , methanol (HPLC degree) and chloroform (ACS grade) were obtained from Carlo Erba (Milan, Italy).

Peptide R Synthesis and Purification

Peptide R, antagonist of CXCR4 (Arg-Ala-[Cys-Arg-Phe-Phe-Cys]) was synthesized on solid phase by using Fmoc chemistry standard protocols [19, 20]. Briefly, the peptide cleavage from the solid support and the deprotection of all amino acid residues were obtained upon treatment with high percentage of trifluoroacetic acid, H2O and triisopropylsilane (TFA/H2O/EDT 94:4:2). The cyclisation reaction was performed by disulphide bridge formation between two cysteine residues. In particular the oxidation reaction was performed dissolving the crude products in aqueous solution (0.1 M) of NH4HCO3. The compound was obtained in good yield and with high purity grade (>95%) after RP-HPLC purification. It was fully characterized for its identity by mass spectrometry.

Liposomes preparation

Liposomes composed of DPPC:Chol:DSPE-PEG2000 or DPPC:Chol:DSPE-PEG-Mal at a 65:30:5 molar ratio were prepared by hydration of thin lipid film followed by extrusion. Briefly, lipids were

dissolved in chloroform/methanol (2:1 v/v) and placed in round-bottom flask under nitrogen atmosphere; the solvent was removed under vacuum in a rotary evaporator (Laborota 4010 digital, Heidolph, Schwabach, Germany). The resulting lipid film was rehydrated with citrate buffer at pH 4 (150 mM sodium citrate; 150mM citric acid), at 50°C for 2 h. The liposome suspension was then extruded at 50°C, using a thermobarrel extruder system (Northern Lipids Inc., Vancouver, BC, Canada). The liposomal suspension was repeatedly passed through polycarbonate membrane (Nucleopore Track Membrane 25mm, Whatman, Brentford, United Kingdom) with 0.1 μm pore size. The external buffer was removed by ultracentrifugation (Optima Max E, Beckman Coulter, USA; rotor TLA 120.2) at 80.000 rpm, at 4°C for 40 min, and the liposomes were re-suspended with 1 ml of HBS buffer at pH 7.4 (140mM sodium chloride; 25mM of HEPES; 0.1mM of EDTA). DOX was encapsulated into liposomes by remote loading as described previously [29]. Briefly, the liposome suspension was combined with the doxorubicin at a drug/lipid ratio of 0.2 (w/w), and then incubated at 65°C for 1 h. Un-encapsulated DOX was removed by ultracentrifugation 80.000 rpm at 4°C for 30 min. Purified liposomes were re-suspended in HBS buffer. To prepare liposomes conjugated with the anti-CXCR4 peptides, formulations containing DSPE-PEG-Mal were used. Briefly, thiolated derivatives of Peptide R were obtained by reacting the peptide with 2-iminothiolane at 1:10 molar ratio in HBS buffer at pH 8, with gentle magnetic agitation at room temperature for 1 h. The thiolated peptides was purified by Sephadex G-25 (in HBS buffer pH 6.5). The peptide (100 μM) was conjugated to liposomes containing DSPE-PEG-Mal at room temperature, overnight. The resulting liposomes were than chromatographed on a Sepharose CL-4B column in HBS buffer pH 7.4. For the in vivo experiments, liposomes encapsulating DOX were prepared at the final concentration of about 0.29 mg/ml, and 0.05 mg/ml of DPPC and DOX, respectively; in the case of Peptide R-modified liposomes encapsulating DOX, a formulation at the final concentrations of about 0.29 mg/ml, 0.01 mg/ml and 0.05 mg/ml of DPPC, Peptide R and

DOX, respectively, was prepared. All the formulations were opportunely diluted before use. All liposome preparations were stored at 4°C. The formulations were prepared in triplicate.

Liposomes characterization

The mean diameter and size distribution of liposome, were measured by photon correlation spectroscopy (PCS) (N5, Beckman Coulter, Miami, USA) at 20°C. Each sample was diluted in deionizer/filtered (0.22µm pore size, polycarbonate filters, MF-Millipore, Microglass Heim, Italy) water and analyzed with detector at 90° angle. The particle size distribution was expressed as polydispersity index (P.I.). For each batch, mean diameter and size distribution were the mean of three measures. For each formulation, the mean diameter (reported in nm) and P.I. were calculated as the mean of three different batches. The zeta-potential (ζ) of the liposomes surface was measured following dilution in water by means of a ZetasizerNano Z (Malvern, UK). Data of ζ were collected as the average of 20 measurements. DOX encapsulation into liposomes was determined by dosing the un-encapsulated drug. Briefly, supernatants were carefully removed and DOX concentration was determined by UV/Visible Spectrophotometer at 480 nm. The results have been expressed as encapsulation efficiency, calculated as $[(TS_{DOX} - AS_{DOX})/ TS_{DOX}] \times 100$, where TS_{DOX} is the theoretical DOX concentration in the supernatant before encapsulation and AS_{DOX} is the actual DOX concentration found in the supernatant.

Cell Culture

A498, human renal cancer cell line, HT29, colon cancer cell line and FB-1 human anaplastic thyroid cancer cell line, were grown at 37°C in 5% CO_2 in DMEM (Dulbecco's Modified Eagle Medium) with 10% fetal bovine serum (FBS), 2 mM glutamine, 1 mM sodium pyruvate, 50 µg/mL penicillin, 50 µg/mL streptomycin. B16-CXCR4 murine melanoma cell line transfected with CXCR4 [20] was grown at 37°C in 5% CO_2 in IMDM (Iscove Modified Dulbecco's Medium) with 10% FBS and 2mM glutamine, 50 µg/mL penicillin, 50 µg/mL streptomycin and 2 mg/mL G418.

B16 cells were transfected with CXCR4 according to FuGENE 6 protocol (Roche Applied Science, Indianapolis, IN). All the tested cell lines were morphologically identified monthly.

Cytotoxicity assay

Cells were plated in 96-well plates (1500 cells/well) and three-day cytotoxicity assays were performed using the Sulphorhodamine B (SRB) assay. Cells fixed with 10% ice-cold trichloroacetic acid at 4°C for 1 h were washed and dried at room temperature. The cellular proteins in each well were stained with 100 µl of 0.4% SRB in 1% acetic acid at room temperature for 30 min and then washed with 1% acetic acid four times and dried at room temperature. To dissolve the SRB bound to cellular protein, 200 µl of 10 mM Tris were added to each well. SRB bound to protein was measured by absorbance at a 540-nm wavelength.

Real Time PCR

Total RNA from cells were extracted using RNeasy Mini Kit quick spin columns (Qiagen), according to the manufacturer's instructions. DNase-treated RNA (200 ng) was reverse transcribed by Superscript II RNase H-reverse transcriptase according to the manufacturer's instructions (Invitrogen-Life Technologies, Carlsbad, CA, USA). Real time-PCR was carried out using about 10 ng of cDNA in 25 µl final of SYBR Green reaction mixture. An ABI Prism 7000 (Applied Biosystems) robocycler was used for the amplification. For CXCR4, cycling conditions of the PCR were as follows: initial denaturation (10 min at 95°C) followed by 40 cycles of denaturation (15 s at 95°C), annealing (30 s at 60°C) synthesis (1 min at 72°C), followed by final extension (7 min at 72°C). The gene-specific primers used for the amplification were as follows: CXCR4: 5'-TGAGAAGCATGACGGACAAG-3' (forward); 5'-AGGGAAGCGTGATGACAAAG-3' (reverse); GUSB: 5'-AGCCAGTTCCTCATCAATGG-3' (forward); 5'-GGTAGTGGCTGGTACGGAAA-3' (reverse). Subsequently, CXCR4 mRNA was quantified comparing its expression to GUSB mRNA levels. Samples were run in triplicate.

Quantification of CXCR4 Surface Expression

Cells ($1x10^6$) were harvested and rinsed twice, and 1% bovine serum albumin (BSA) in PBS solution was used to block the cells for 30 min in an ice bath. Then cells were stained with anti-CXCR4 PE-antibody (FAB170P, clone 12G5, R&D Systems, Minneapolis, MN, USA) for 1 h at 4°C. After antibody staining, cells were rinsed with 1% BSA in PBS three times, resuspended in PBS, and evaluated by a FACS Canto II cytofluorometer (Becton Dickinson Immunocytometry Systems, Mountain View, CA, USA).

CXCR4 Immunofluorescence

Cells (1×10^4) were seeded on glass coverslips, after 24h were fixed with 4% paraformaldehyde (15 min, 4°C) and blocked with 1% BSA in PBS for 30 min in an ice bath. Resulting fixed cells were stained with mouse anti-human CXCR4 primary antibody (clone 12G5 R&D) and Alexa Fluor goat anti-mouse 488-conjugated secondary antibody, sequentially. DAPI was used to stain the cell nucleus. Samples were examined under a fluorescent microscope (Carlo Zeiss, Axio Scope.A1).

***In vitro* cellular uptake study by FACS analysis**

The inherent fluorescence of doxorubicin (DOX) (excitation 480 nm, emission 575 nm) was used to evaluate the intracellular DOX concentration using flow cytometry. Cells were incubated in growing media with free DOX, PL-PeptideR-DOX, PL-DOX for 4 or 24 hours at 37 °C and immediately analyzed with FACS Canto II cytofluorometer (Becton Dickinson Immunocytometry Systems, Mountain View, CA, USA). DOX molecular associated with cells was excited with an argon laser (488 nm) and the emitted fluorescence detected through 575 nm band pass filter.

Migration assay

Migration was assayed in 24 Transwell chambers (Corning Inc., Corning, NY) using inserts with 8-µm pore membrane. A498, HT29, B16-CXCR4 and FB-1 cells were placed in the upper chamber (2×10^5cells/well) in DMEM containing 0.5% BSA (migration media) in the presence of either AMD3100, Peptide R, PL-Peptide R, PL. 100 ng/mL CXCL12 was added to the lower chamber. After 18 hours of incubation, cells on the upper surface of the filter were removed using a cotton

wool swab; the cells that had migrated onto the lower surface of the membrane were stained with DAPI, photographed and visually counted in 10 random fields. Migration index is the ratio between number of migrated cells / number of migrating cells toward CXCL12 free media.

In vivo Metastases Assay

Twenty 6-8-week-old female C57BL/6 mice (Harlan) were inoculated into the tail vein with 5 x 10^5 B16–CXCR4 cells. The following day mice (5/group) were divided into four groups according to the following treatments: PBS, Peptide R (0.1mg/Kg), PL-Peptide R (0.1 mg/Kg) where the dose in mg/kg is referred to Peptide R, PL; an amount of liposomes equivalent to that of PL-Peptide R was used. Mice were treated twice/ week intravenously for 2 weeks.

Histological evidence of metastases was obtained with a computer-assisted image measurement program by a microscope (BX51 microscope and DP-1 microscope digital camera; Olympus Japan). Lungs were harvested 21 days post-cell injection. The tissues were stained as follow: Mice derived lungs were fixed in 10% buffered formalin, paraffin-embedded and subsequently sectioned into 3-µm slices. The sections were stained with haematoxylin/eosin to evaluate metastasis [(one-way ANOVA) followed by Bonferroni's post test was performed using SPSS version 13 (IBM SPSS Statistics)]. The Istituto Nazionale per lo Studio e la Cura dei Tumori, Fondazione Giovanni Pascale Independent Ethical Comettee approved the study and experiments were performed in accordance with the Institutional Animal Care and Use Committee guidelines. Kaplan-Meier analysis was conducted for 8 mice/group.

The delivery of DOX by PL-Peptide R-DOX versus PL-DOX was evaluated. B16-CXCR4 cells (5 x 10^5) were injected into the tail vein of fifteen C57BL/6 female mice. The following day mice (5/group) were divided in groups as follows: PBS; PL-DOX 0.5 mg/kg where the dose in mg/kg is referred to Doxorubicin; and PL-Peptide R 0.1mg/Kg- DOX 0.5 mg/kg where the dose in mg/kg is referred respectively to Peptide R(0.1mg/Kg) and Doxorubicin 0.5 mg/kg (200 µl of PL-DOX or PL-Peptide R-DOX iv twice/week for two weeks). Lungs were harvested 21 days post-cell injection

and fixed in formalin for H&E staining. Frozen sections were cryo-sectioned using a Cryotome Cryostat, mounted on superfrost plus slides, treated with DAPI for 15 min, washed and and observed by confocal microscope (LSM 510 Zeiss). Approximately 50 cells per microscopic field were observed in each sample and at least 3 field for each sample were analyzed. Fluorescence intensity was calculated by LSM 510 Zeiss softwere, averaging the fluorescence intensity of each pixel in the miscroscopic field.

Statistical Analysis.

The values given are means ± standard deviation. Student's t-test was used for comparing the means and differences with a P value of < 0.05 were considered significant.

Results

Characterization of Liposomes and Peptide R.

Peptide R is a 7 amino acids - cyclic -peptide[20] with migration IC_{50} of 51 ± 6 nM in human renal cancer cells (Supplementary Figure 1). Peptide R was conjugated with the PEG chain on the surface of preformed liposomes (PL-Peptide R). The characteristics of the PL-Peptide R are summarized in Table 1. Liposomes with a mean diameter ranging from about 130 to 140 nm were prepared. Conjugation with the peptide did not significantly affect the mean diameter of the liposomes (Table 1). The formulation was characterized by a narrow size distribution with a PI always below a value of 0.2. Blank PEGylated liposomes (PL) were characterized by a slightly negative zeta potential, which significantly decreased following conjugation with the peptide. PEGylated liposomes encapsulating DOX (PL-DOX) and Peptide R-conjugated PEGylated liposomes encapsulating DOX (PL-Peptide R-DOX) were also prepared. In both cases, DOX was loaded at a drug/lipid ratio of about 0.184 (w/w), corresponding to a DOX encapsulation efficiency of about 92% (Figure 1).

PL-Peptide R inhibited CXCL12-induced migration in CXCR4 expressing human cancer cells.

CXCR4 expression was characterized in HT29, human colon cancer and A498, human renal cancer cells. As shown in Figure 2A-C, HT29 and A498 cells expressed CXCR4 at the RNA and protein level while FB-1, human anaplastic thyroid cancer cells, expressed very low level of CXCR4 [30]. The Peptide R was previously shown to inhibit CXCR4-dependent migration, ligand binding, P-ERK1/2-induction and calcium efflux. Moreover Peptides R drastically reduced the number of K7M2 osteosarcoma and B16-CXCR4-derived lung metastases and the growth of a renal cells xenograft[20]. To evaluate the effect of PL-Peptide R on cell migration, CXCR4 expressing cells (A498 and HT29) were incubated in the presence of PL-Peptide R or Peptide R and allowed to migrate toward CXCL12-containing media. As previously demonstrated[20] Peptide R significantly inhibited CXCR4 positive cells migration. PL-Peptide R inhibited CXCL12-induced migration *in*

vitro in CXCR4 expressing cells more efficiently than Peptide R alone (PL-Peptide R versus Peptide R exhibited 2.3 vs 1.6 migration fold reduction). FB-1 cells, expressing low level of CXCR4, did not migrate toward CXCL12.

PL-Peptide R reduced lung metastases and increased survival in B16-CXCR4 C57BL/6 mice.

B16-CXCR4 melanoma cells derived lung metastasis were previously reported to be inhibited by Peptide R [20]. In Figure 3A it is shown that B16-CXCR4 expressed higher CXCR4 compared to B16 cells. In Figure 3B, B16-CXCR4 cells migration toward CXCL12, in the presence of PL or Peptide R or PL- Peptide R, was shown; a lower number of B16-CXCR4 cells migrated toward CXCL12 when treated with PL-Peptide R compared to Peptide R alone (3.7 versus 1.7 fold by PL- Peptide R versus Peptide R). For the in vivo experiment, 5×10^5 murine melanoma B16-CXCR4 cells were injected into the tail vein of C57BL/6 mice. Mice were treated twice/week for two weeks intravenously with Peptide R (0.1 mg/Kg), PL-Peptide R (0.1 mg/Kg) or PL-liposome. In Figure 4A, treatment with PL-Peptide R significantly reduced B16-CXCR4 lung metastases compared to treatment with Peptide R ($P = 0.02$). Interestingly, this efficient reduction in metastases development was observed with 0.1mg/kg of Peptide R, 1/20 dose previously evaluated to be efficient (2 mg/kg) intraperitoneally for 10 days in the same experimental setting [20]. Moreover PL-Peptide R treated mice exhibited prolonged survival compared to mice treated with Peptide R alone (Figure 4B). No signs of toxicity were observed.

Targeting of CXCR4 by PL Peptide R loaded with doxorubicin.

To demonstrate that targeting CXCR4 expressing cells through PL-Peptide R represents also a modality to deliver agents to CXCR4 expressing cells, the PL-Peptide R was loaded with doxorubicin (DOX) (Table 1). Since exposure to its ligands [31] and/or exposure to selective antagonists [32] results in rapid CXCR4 receptor internalization, PL-Peptide R could favor the delivery of doxorubicin into the target cells [33, 34]. To evaluate the improvement in CXCR4 targeting specificity induced by Peptide R, cellular uptake of PL-Peptide R-DOX was compared to PL-DOX

and free DOX in HT29 and FB-1 cells (Figure 5A). As shown in Figure 5A, intracellular doxorubicin was significantly higher in HT29 cells exposed to PL-Peptide R-DOX compared to PL-DOX while the intracellular doxorubicin was comparable in FB-1 cells exposed to either PL-Peptide R-DOX or PL-DOX, suggesting that the specific CXCR4 targeting increased doxorubicin accumulation in CXCR4 expressing cells. As an effect of drug delivery increased doxorubicin cytotoxicity was registered. In Table 2, PL-Peptide R-DOX treatment compared to PL-DOX lowered doxorubicin IC_{50} in HT29 and in A498 cells.

Higher doxorubicin was detected in pulmonary metastasis of B16-CXCR4-PL-Peptide R-DOX-treated mice compared to PL-DOX (Figure 6A). PL-Peptide R-DOX treatment efficiently reduced lung metastasis number and dimension compared to PL-DOX treatment (Figure 6 B-C).

Discussion

While targeting solid tumors with nanomedicine is a consolidated approach, the use of anti-metastasis nanomedicines is gaining attention [35-37]. Liposomes offer multiple advantages including the modulation of the outside surface of liposome with targeting molecules to improve the antimetastatic efficacy [37]. CXCR4-CXCL12 signaling favors metastasis in diverse experimental settings [18] and recently, a novel class of CXCR4-antagonist cyclic peptides was developed [20]. Unfortunately, the therapeutic use of peptides is questionable due to short in vivo half-life as well as aspecific distribution into the body and plasmatic protein binding [38]. To improve efficacy of Peptide R, PEGylated liposomes conjugated to Peptide R were designed and tested in vitro and in vivo. As previously found for other peptides and proteins [39], the chemical modification with PEG, reasonably on the N-terminal of the peptide (although the reaction with other primary amino groups of lateral chains of arginine and alanine cannot be excluded), did not affect Peptide R activity.

PL-Peptide R inhibited CXCL12-induced migration *in vitro* in CXCR4 expressing cells more efficiently than Peptide R alone. The increased activity of PL-Peptide R compared to peptide alone could be explained with the multivalency of targeted liposomes. Conjugation of multiple copies of a ligand to the surface of a nanoparticle will impart multivalent binding with a more potent interaction of the ligand for its target, as previously reported [40,41]. Furthermore, PL-Peptide R impaired CXCR4 function *in vivo* more efficiently than Peptide R by reducing B16-CXCR4 lung metastasis and increasing life span in immunocompetent mice. In contrast with the previous *in vivo* experiments conducted in the same setting, in which Peptide R was administered intraperitoneally at the dose of 2 mg/kg for 10 days [20], PL-Peptide R was administered intravenously at the dose of 0.1 mg/kg twice a week for two weeks. Thus, PL-Peptide R decreased B16-CXCR4 lung metastases even with a 1/20 of the dose of Peptide R previously used [20], while in the same conditions the free Peptide R was not active. To justify this observation we assume that the conjugation of Peptide R with liposomes could prolong the blood residence of the active peptide in the plasma. Preliminary

evidences showed that PL-Peptide R displayed a higher stability in plasma compared to unconjugated Peptide R (Supplementary Figure 2). Based on that, these nanocarriers were also evaluated for deliver specificity. Doxorubicin was taken into account as model chemotherapeutic and encapsulated into the PL-Peptide R by remote loading [42]. The DOX encapsulation into the liposomes lead to a slight increase of the mean size, reasonably attributed to the remote loading method that produce DOX precipitates into the vesicles[43]. An increase of the PI was detected in the formulation PL-Peptide R, upon the encapsulation of DOX possibly due to a PL-Peptide R additional preparation and purification step (including the heating at 65°C) that could slightly affect the liposome size distribution. *In vitro* studies demonstrated that PL-Peptide R-DOX specifically accumulated in CXCR4 expressing cells through CXCR4 receptor binding and internalization, as reported for the endogenous ligand or/and the CXCR4 inhibitor, AMD3100 [31, 32]. CXCR4 surface density predicted enhanced binding and cytotoxicity; in accordance with this, higher amount of doxorubicin penetrated in B16-CXCR4 and HT29 treated with PL-Peptide R-DOX decreasing the doxorubicin $IC_{50.}$

Another peptide belonging to the Peptide R family, Peptide S, was recently. co-administered with DOX-encapsulating liposomes [44]; the authors demonstrate that fibroblast derived-CXCL12 is antagonized by Peptide S that, disrupting adhesion between B16F10 cells and stromal cells, release the B16F10 cells from the stromal anchorage. In this modality the cells are more prone to chemotherapeutics effect demonstrating another effect of CXCR4 antagonism [44]. Li et al developed an AMD3100-based polycations with dual-function: prevent cancer cell invasion by inhibiting CXCL12-stimulated CXCR4 activation, and efficiently and safely deliver plasmid DNA into cancer cells. This interesting study represents for us a proof of principle for combined therapy on a CXCR4 targeting nanocarrier [45]. Our study proposes a nanocarrier to optimize the biopharmaceutical profile of the new developed CXCR4-targeting Peptide R, a not toxic and efficient CXCR4 antagonist in clinical development. In addition, the CXCR4-targeting peptide liposomes (PL-Peptide R) could

favor the delivery of encapsulated agents, e.g. a chemotherapeutic such as doxorubicin (DOX), into the CXCR4 expressing target cells. In the present study, we combined the use of the CXCR4-antagonist peptide and the DOX-encapsulating liposomes in the same product and demonstrated the in vivo targeting of CXCR4 expressing lung metastasis. In addition, since PL-peptide R efficiently deliver DOX in CXCR4-rich melanoma lung metastasis, this system can be successfully used as CXCR4-targeted delivery systems, providing the proof-of-concept for a combination therapy. Similarly, liposomes were proposed to deliver combination therapies based on timing and sequence of drug release such as naturally hydrophobic (erlotinib, afatinib, gefitinib, and lapatinib) or hydrophilic (doxorubicin and cisplatin) drugs [46]. However, in this study, one of the two active entities also works as ligand for targeted drug delivery of drugs. This approach allows to reduce the preparation steps of the final product, as well as the number of chemical entities to achieve a combined therapy together with a targeted delivery of the chemotherapeutics.

Conclusions

In conclusion liposomes conjugated-Peptide R potentiate Peptide R efficacy and allow specific distribution into CXCR4 overexpressing tumours. PL-Peptide R-DOX, beyond its antagonistic CXCR4 activity, efficiently deliver doxorubicin in melanoma lung metastasis. This nanocarrier is providing combined functions: antimetastatic active agent, as CXCR4 antagonism reduces metastases formation, and drug delivery system, as CXCR4 antagonist-expressing liposomes specifically deliver doxorubicin to CXCR4 expressing tumor providing the proof-of-concept for a combination therapy [46].

Competing interests

The authors declare that they have no competing interests.

Acknowledgments

This work was supported by a grant of the Associazione Italiana per la Ricerca sul Cancro (AIRC) IG n. 13192.

References

[1] J.A. Burger, T. J. Kipps, *Blood*, 2006, **107**, 1761–1767.

[2] M. Darash-Yahana, E. Pikarsky, R. Abramovitch, E. Zeira, B. Pal, R. Karplus, K. Beider, S. Avniel, S. Kasem, E. Galun, A. Peled, *FASEB J.* 2004, **18**, 1240-1242.

[3] A. Ottaiano, R. Franco, A. Aiello Talamanca, G. Liguori, F. Tatangelo, P. Delrio, G. Nasti, E. Barletta, G. Facchini, B. Daniele, A. Di Blasi, M. Napolitano, C. Ieranò, R. Calemma, E. Leonardi, V. Albino, V. De Angelis, M. Falanga, V. Boccia, M. Capuozzo, V. Parisi, G. Botti, G. Castello, R. Vincenzo Iaffaioli, S. Scala, *Clin Cancer Res*. 2006, **12**, 2795-2803.

[4] F. Marchesi , P. Monti, B. E. Leone, A. Zerbi, A. Vecchi, L. Piemonti, A, Mantovani, P. Allavena, *Cancer Res.* 2004, **64**, 8420-8427.

[5] C. D'Alterio , C. Consales, M. Polimeno, R. Franco, L. Cindolo, L. Portella, M. Cioffi, R. Calemma, L. Marra, L. Claudio, S. Perdonà, S. Pignata, G. Facchini, G. Cartenì, N. Longo, L. Pucci, A. Ottaiano, S. Costantini, G. Castello, S. Scala, *Curr Cancer Drug Targets,* 2010, **10**, 772-781.

[6] S. Scala, P. Giuliano, P.A. Ascierto, C. Ieranò, R. Franco, M. Napolitano, A. Ottaiano, M.L. Lombardi, M. Luongo, E. Simeone, D. Castiglia, F. Mauro, I. De Michele, R. Calemma, G. Botti, C. Caracò, G. Nicoletti, R.A. Satriano, G. Castello, *Clin Cancer Res.* 2006, **12**, 2427-2433

[7] C. D'Alterio , A. Barbieri, L. Portella, G. Palma, M. Polimeno, A. Riccio, C. Ieranò, R. Franco, G. Scognamiglio, J. Bryce, A. Luciano, D. Rea, C. Arra, S. Scala, *Cancer Immunol Immunother.* 2012, **61**, 1713-1720.

[8] D. Mukherjee, J. Zhao, *Am. J. Cancer Res.* 2013, **3**, 46-57.

[9] S. Scala. *Clin Cancer Res.* 2015, DOI: 10.1158/1078-0432.

[10] L. Patrussi, C.T. Baldari, *Curr Med Chem.* 2011, **18**, 497-512.

[11] U.M. Domanska , R.C. Kruizinga, W.B. Nagengast, H. Timmer-Bosscha, G. Huls, E.G. de Vries, A.M. Walenkamp, *Eur J Cancer,* 2013, **49**, 219-230.

[12] M.P. Rettig, G. Ansstas, J.F. Di Persio, *Leukemia*, 2012, **26**, 34-53.

[13] E. De Clercq, *Biochem Pharmacol.* 2009, **77**, 1655-1664.

[14] J.F. Di Persio, E.A. Stadtmauer, A. Nademanee, I.N. Micallef, P.J. Stiff, J.L. Kaufman, R.T. Maziarz, C. Hosing, S. Früehauf, M. Horwitz, D. Cooper, G. Bridger, G. Calandra, *Blood,* 2009, **113**, 5720-5726.

[15] M.R. Kuhne, T. Mulvey, B. Belanger, S. Chen, C. Pan, C. Chong, F. Cao, W. Niekro, T. Kempe, K.A. Henning, L.J. Cohen, A.J. Korman, P.M. Cardarelli, *Clin Cancer Res.* 2013, **19**, 357-366.

[16] K. Kashima, M. Watanabe, Y. Sato, J. Hata, N. Ishii, Y. Aoki, *Cancer Science,* 2014, **105**, 1343-1350.

[17] S.B. Peng , X. Zhang, D.Paul , L.M. Kays, W. Gough, J. Stewart, M.T. Uhlik, Q. Chen, Y.H. Hui, M. J. Zamek-Gliszczynski, J.A. Wijsman, K.M. Credille, L.Z.Yan, *Mol Cancer Ther.* 2014, DOI:10.1158/1535-7163.

[18] B. Debnath, S. Xu, F. Grande, A. Garofalo, N. Neamati, *Theranostics,* 2013, **3**, 47-75.

[19] P. Amodeo, R.M. Vitale, S. De Luca, S. Scala, G. Castello, A. Siani, Italian patent: no. MI2010A 000093; International patent n° WO2011/092575 A, 2010.

[20] L. Portella , R. Vitale, S. De Luca, C. D'Alterio, C. Ieranò, M. Napolitano, A. Riccio, M.N. Polimeno, L. Monfregola, A. Barbieri, A. Luciano, A. Ciarmiello, C. Arra, G. Castello, P. Amodeo, S. Scala, *PLoSOne*, 2013, **8**, e74548.

[21] B. J. Bruno, G. D. Miller, C. S. Lim, *Therapeutic Delivery*, 2013, **4**, 1443-1467.

[22] R.O. Dillman, *Cancer Invest.* 2001, **19**, 833-841.

[23] A.W. Du, M.H. Stenzel, *Biomacromolecules* 2014, **15**, 1097-1114.

[24] P. Guo, J.O. You, J. Yang, M.A. Moses, D.T. Auguste, *Biomaterials*, 2012, **33**, 8104-8110.

[25] P Guo, J.O. You, J. Yang, D. Jia, M.A. Moses, D.T. Auguste, *Mol Pharm.* 2014, **11**, 755-765.

[26] C. Chittasupho, K. Lirdprapamongkol, P. Kewsuwan, N. Sarisuta, *Eur J Pharm Biopharm.* 2014, **88**, 529-538.

[27] V. Sanna, N. Pala, M. Sechi, *Int. J. Nanomedicine,* 2014, **9**, 467-483.

[28] D.B. Fenske, A. Chonn, P.R. Cullis, *Toxicol. Pathol*. 2008, **36**, 21-29.

[29] L.D. Mayer, M.B. Bally, P.R. Cullis. *Biochim Biophys Acta*, 1986, **857**, 123-126.

[30] V. De Falco, V. Guarino, E. Avilla, M.D. Castellone, P. Salerno, G. Salvatore, P. Faviana, F. Basolo, M. Santoro, R.M. Melillo, *Cancer Res.* 2007, **67**, 11821-11829.

[31] A. Marchese, *Curr Opin Cell Biol.* 2014, **27**, 72-77.

[32] K. Hattermann, E. Holzenburg, F. Hans, R. Lucius, J. Held-Feindt, R. Mentlein, *Cell Tissue Res.* 2014, **357**, 253-266.

[33] V. Vichai, K. Kirtikara, *Nature Protocols,* 2006, **1**, 1112-1116.

[34] D.B. Kirpotin, D.C. Drummond, Y. Shao, M.R. Shalaby, K. Hong, U.B. Nielsen, J.D. Marks, C.C. Benz, J.W. Park, *Cancer Res.* 2006, **66**, 6732-6740.

[35] S. Bhana, Y. Wang, X. Huang, *Nanomedicine (Lond)*, 2015, **10**, 1973-1990.

[36] P. Xu, Q. Meng, H. Sun, Q. Yin, H. Yu, Z. Zhang, M. Cao, Y. Zhang, Y. Li, *Biomaterials,* 2015, **64**, 10-20.

[37] Q. He, S. Guo, Z. Qian, X. Chen, *Chem. Soc. Rev.* 2015 DOI 10.1039/C4CS00511B

[38] A. Peled, M. Abraham, I. Avivi, J.M. Rowe, K. Beider, H. Wald, L. Tiomkin, L. Ribakovsky, Y. Riback, Y. Ramati, S. Aviel, E. Galun, H.L. Shaw, O. Eizenberg, I. Hardan, A. Shimoni, A. Nagler, *Clin Cancer Res.* 2014, **20**, 469-479.

[39] C. Ginn, H. Khalili, R. Lever, S. Brocchini. *Future Med Chem*. 2014, **6**, 1829-46

[40] R. Weissleder, K., E.Y Sun, T. Shtatland, L. Josephson. *Nat Biotechnol.* 2005*,* **23,** 1418–1423

[41] R. Hennig, K. Pollinger, A. Veser, M. Breunig, A. Goepferich. *J Control Release*. 2014, **28,** 194:20-7.

[42] A. Fritze, F. Hens, A. Kimpfler, R. Schubert, R. Peschka-Suss, *Biochim Biophys Acta,* 2006, **1758**, 1633-1640.

[43] G. Haran, R. Cohen, LK. Bar, Y. Barenholz. *Biochim Biophys Acta*. 1993, **2,** 201-15

[44] L. Mei, Y. Liu, Q. Zhang, H. Gao, Z. Zhang, Q. He, *Journal of Controlled Release,* 2014, **196**, 324-331.

[45] J. Li J, Y. Zhu, S.T. Hazeldine, C. Li, D. Oupický. *Angew Chem Int Ed Engl.,* 2012 ,**35,** 8740-3.

[46] S.W. Morton, M. J. Lee, Z.J. Deng, E. C. Dreaden, E. Siouve, K. E. Shopsowitz, N. J. Shah, M.B. Yaffe, P. T. Hammond, *Science Signaling*, 2014, **7**, ra44.

Figure Legends

Figure 1. Characterization of PL-Peptide R. Schematic illustration of the different formulations/treatments tested in this study.

Figure 2. PL-Peptide R inhibited CXCL12-induced cell migration in CXCR4 expressing human cancer cells. (A) CXCR4 gene expression by qRT-PCR. CXCR4 fold chan**ge i**s relative to GAPDH. CCRF-CEM, a human T-lymphoblast cell line, was used as CXCR4 positive control. (B) CXCR4 surface expression in HT29, A498 and FB-1 cells via flow cytometry. Histograms show the mean fluorescence intensities (MFI) of cells stained with PE-conjugated-IgG as controls (left panel) and PE-conjugated anti-CXCR4 antibody (right panel). (C) Representative fluorescence microscope images of CXCR4 in HT29, A498 and FB-1 cells. DAPI was used to stain the cell nuclei; mouse anti-human CXCR4 antibody (primary) and Alexa Fluor 488-conjugated goat anti-mouse antibody (secondary) were used to assess CXCR4 expression. A498shCXCR4 cells, A498 stably silenced with short harpin RNA antiCXCR4, were used as the CXCR4 negative control. (D) CXCL12 dependent-cell migration was examined in A498, HT-29 and FB-1 in 24-well plates. Cells migrated toward CXCL12 (100ng/ml) for 18 hours. The cells were counted in ten different consecutive high power fields (magnification 200X). The results are expressed as the migration index respect to migration in presence of CXCL12 alone. Each column represents the mean ± S.D. (n=3). Statistical significances were calculated by Student's t-test. * $p<0.05$, ** $p<0.01$ CXCL12 *vs* BSA; PL-Peptide R *vs* CXCL12.

Figure 3. PL-Peptide R inhibited CXCL12-induced cell migration in B16-CXCR4 murine melanoma cells. (A) Cell surface expression of CXCR4 was determined by flow cytometry on transfected B16 murine melanoma cells (B16-CXCR4). (B) Cells were plated on a membrane in a medium containing PL, Peptide R, PL- Peptide R toward a CXCL12 medium as source of chemoattractant. After 18 hours of incubation, the cells that had migrated onto the lower surface of the membrane were stained with DAPI and visually counted in 10 random fields (upper panel).

Representative images of B16-CXCR4 cells migration after treatment with Peptide R, PL and PL-Peptide R (upper panel). The effects of Peptide R, PL and PL-Peptide R on migration of B16-CXCR4 cells (lower panel). Each column represents the mean ± S.D. (n=3). Statistical significances were calculated by Student's t-test. **p<0.01 CXCL12 *vs* BSA; Peptide R *vs* CXCL12; PL-Peptide R *vs* CXCL12.

Figure 4. PL-Peptide R reduced B16-CXCR4 lung metastases development and increased survival. (A) Mice lungs treated with PBS, liposome unconjugated (PL), Peptide R [0.1mg/Kg] (Peptide R) and PL-Peptide R [0.1mg of peptide/Kg] (PL-Peptide R) (left panel). Graphical representation of lung metastases number in treated mice. Double tailed T-Test was used for statistical analyses. Differences were considered significant at P<0.05 compared to control (right panel). (B) Kaplan-Meier survival curves of C57BL/6 mice that were treated as above.

Figure 5. PL-Peptide R increased doxorubicin internalization in CXCR4 positive cell lines. (A) Cellular uptake of PL-DOX and PL-Peptide R-DOX in HT29 and FB-1 cells by flow cytometry. Black curve represents negative control; Red curve represents the fluorescence of cells incubated with DOX; Blue curve represents the fluorescence of cells incubated with PL-Peptide R-DOX; Green curve represents the fluorescence of cells incubated with PL –DOX. In HT29 the MFI (mean fluorescence intensity) of PL-Peptide R-DOX vs PL-DOX was 4±0.2 vs 2.1±0.1; $P < 0.05$. (B) Representative histograms of B16-CXCR4 cells incubated with DOX, PL-DOX and PL-Peptide R-DOX (doxorubicin dose 0.5ug/ml for 4 and 24 hours). Black curve represents negative control; Red curve represents the fluorescence of cells incubated with DOX; Blue curve represents the fluorescence of cells incubated with PL-Peptide R-DOX; Green curve represents the fluorescence of cells incubated with PL –DOX. The amount of doxorubicin (MFI) was 1.7 ± 0.1 and 2.9 ± 0.3 at 4 hours and 2.6 ± 0.5 and 22 ± 0.90 at 24 hours of treatment with PL-DOX and PL-Peptide R-DOX, respectively.

Figure 6. PL-Peptide R specifically delivered doxorubicin to CXCR4 expressing cells in vitro and in vivo. (A) Left panel. In vivo doxorubicin delivery of PL-Peptide R-DOX versus PL-DOX. Lung metastases were analyzed by confocal laser scanning microscopy after treatment with PL-Dox (0.5 mg DOX/kg) M3 and PL-Peptide R-Dox (0.5 mg DOX/kg) M6. Right panel. Mean fluorescence intensity by Image J software. The doxorubicin signal was tracked in the red channel (Ex/Em.548/595 nm). Data shown are mean ± SEM of n = 5 mice per group analyzed in two independent experiments. The significance of difference between the mean was analyzed by Student's t-test. (B) Graphical representation of the number of lung metastases in PL-DOX and PL-Peptide R-DOX treated mice. (C) Graphical representation of the pulmonary metastatic tumor dimensions in treated mice. Double tailed T-Test was used for statistical analyses.

Tables

Table1. Characteristics of blank liposomes (BL), liposomes conjugated with Peptide R (PL-Peptide R)*

Formulation	Conjugated peptide	Diameter (nm ± S.D.)	P.I. ± S.D.	ζ (mV) ± S.D.
BL	-	138.9 ± 10.1	0.100 ± 0.05	-6.2 ± 1.5
PL-Peptide R	Peptide R	129.5 ± 13.9	0.103 ± 0.03	-23.8 ± 1.9
PL -DOX	-	154.7 ± 2.9	0.052 ± 0.02	-24.36 ± 1.2
PL-Peptide R-DOX	Peptide R	145.9 ± 4.7	0.286 ± 0.22	-28.88 ± 8.9

***Values are representative of three batches.**

Table2. IC_{50} values (µg/ml) after 72h treatment with Dox, PL-DOX and PL-DOX-Pep R*

Formulation	A498	HT29	FB-1	B16-CXCR4
PL-DOX	40 ± 0.02	20.7 ± 0.025	10.3 ± 0.01	0.46 ± 0.001
PL-Peptide R-DOX	17.9 ± 0.03	6.55 ± 0.04	10.5 ± 0.01	0.2 ± 0.003
DOX	6.01 ± 0.04	1.66 ± 0.03	8.2 ± 0.03	0.31 ± 0.004

***Values are representative of three experiments.**